Computational Geosciences (2006) 10:3–36
DOI: 10.1007/s10596-005-9009-z

Efficient real-time reservoir management using adjoint-based optimal control and model updating

Pallav Sarma[a], Louis J. Durlofsky[a], Khalid Aziz[a] and Wen H. Chen[b]

[a]*Department of Petroleum Engineering, Stanford University, Stanford CA 94305, USA.*
E-mail: lou@stanford.edu
[b]*Chevron Energy Technology Company, San Ramon CA 94583, USA.*

Accepted 8 August 2005

The key ingredients to successful real-time reservoir management, also known as a "closed-loop" approach, include efficient optimization and model-updating (history-matching) algorithms, as well as techniques for efficient uncertainty propagation. This work discusses a simplified implementation of the closed-loop approach that combines efficient optimal control and model-updating algorithms for real-time production optimization. An adjoint model is applied to provide gradients of the objective function with respect to the well controls; these gradients are then used with standard optimization algorithms to determine optimum well settings. To enable efficient history matching, Bayesian inversion theory is used in combination with an optimal representation of the unknown parameter field in terms of a Karhunen–Loeve expansion. This representation allows for the direct application of adjoint techniques for the history match while assuring that the two-point geostatistics of the reservoir description are maintained. The benefits and efficiency of the overall closed-loop approach are demonstrated through real-time optimizations of net present value (NPV) for synthetic reservoirs under waterflood subject to production constraints and uncertain reservoir description. For two example cases, the closed-loop optimization methodology is shown to provide a substantial improvement in NPV over the base case, and the results are seen to be quite close to those obtained when the reservoir description is known a priori.

Keywords: adjoint, Bayesian inversion, closed loop, history matching, Karhunen–Loeve, model updating, optimal control, optimization, reservoir simulation, uncertainty, waterflood

1. Introduction

Real-time model-based reservoir management entails the optimization of reservoir performance under geological uncertainty. For this to be realized in practice, a number of algorithmic advances are required. These include fast optimization procedures, the ability to proficiently incorporate production data to update the reservoir description in real-time, and efficient techniques for treating geological

uncertainty. In this paper, we describe procedures for production optimization and model updating based on the application of optimal control theory, Bayesian inversion theory, and biorthogonal expansions. The propagation of uncertainty is not considered here, although this can be very naturally incorporated into the techniques we present using established methods from other fields [1].

Real-time model-based reservoir management, also referred to as the "closed-loop" approach, can be explained with reference to figure 1. In the figure, the "System" box represents the real system over which some cost function, designated $J(u)$, is to be optimized. In a typical application, $J(u)$ might be net present value (NPV) or cumulative oil produced. The system consists of the reservoir, wells, and surface facilities. Here u is a set of controls including, for example, well rates and bottom hole pressures (BHP), which can be controlled to maximize or minimize $J(u)$. It should be understood that the optimization process results in control of future performance to maximize or minimize $J(u)$, and thus the process of optimization cannot be performed on the real reservoir, but must be carried out on some approximate model. The "low-order model" box represents the approximate model of the system, which – in our case – is the simulation model of the reservoir and facilities. This simulation model is a dynamic system that relates the controls u to the cost function $J(u)$. Since our knowledge of the reservoir is generally uncertain, the simulation model and its output are also uncertain.

The closed-loop process starts with an optimization loop (marked in blue in figure 1 – note that colors refer to the online version) performed over the current

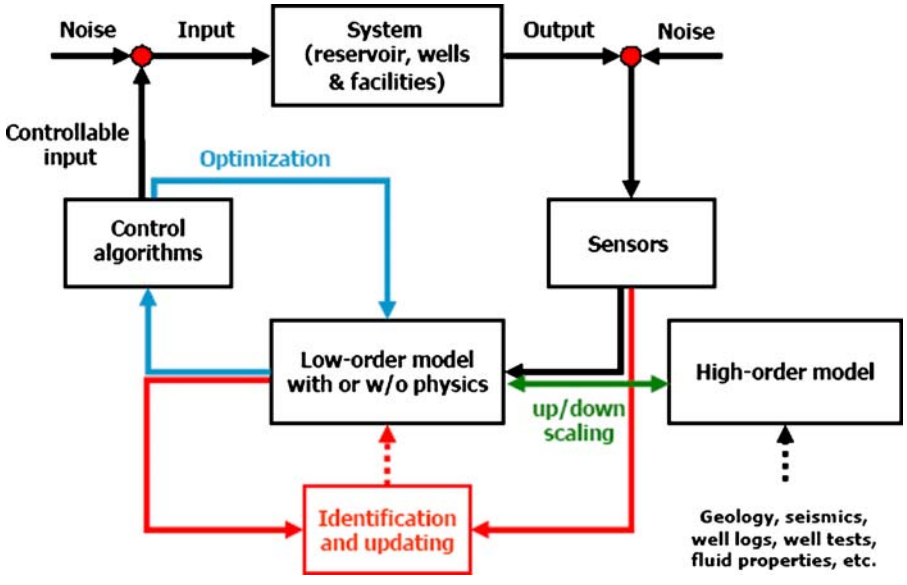

Figure 1. Schematic layout of the closed-loop optimal control approach (from Jansen et al. [3]).

simulation model to maximize or minimize the cost function. This optimization must be performed, in general, on an uncertain simulation model. The optimization provides optimal settings of the controls u for the next control step. These controls are then applied to the real reservoir (as input) over the control step, which impacts the outputs from the reservoir (such as water cuts, BHP, etc.). These measurements provide new information about the reservoir, and therefore enable the reservoir model to be updated (and model uncertainty to be reduced). This is called the model-updating loop, marked in red in figure 1. The optimization loop can then be performed on the updated model over the next control step, and the process repeated over the life of the reservoir.

As indicated above, the closed-loop approach for efficient real-time optimization consists of three key components: efficient optimization algorithms, efficient model-updating algorithms, and techniques for uncertainty propagation. In this work we present a simplified implementation of the closed-loop approach that combines efficient optimal control algorithms and model-updating procedures. Uncertainty propagation is not considered here. Neglecting uncertainty propagation essentially means that the closed-loop process is applied to a single realization of the uncertain parameters; e.g., the maximum likelihood estimate, which is updated at every control step. Such a procedure can be expected to provide near-optimal results in many cases, although the treatment of uncertainty will of course be important in many applications. The entire loop and an application are discussed by Sarma et al. [2].

The key ideas behind closed-loop reservoir management have been known to the oil industry for quite a while, although different names and forms have been used to describe them [3]. Most of the earlier work on closed-loop control was geared toward short-term production optimization, and references for such approaches can be found in [4]. Although relatively little information is required to apply these techniques, long-term production performance is not really optimized as the effect of future events is not taken into account during the optimization process. It has only been recently that closed-loop long-term production optimization has generated some interest. In particular, Brouwer et al. [4] used adjoint models for optimization and Kalman filters for model updating. Adjoint models allow for very efficient optimization, although their implementation can be complicated. The ensemble Kalman filter has only been recently applied for history matching [5]. Although this approach is relatively easy to implement [5, 6], its efficiency compared to established methods such as adjoint models may be an issue. Aitokhuehi and Durlofsky [7] used conjugate gradient algorithms with numerical gradients for optimization and the probability perturbation method [8] for model updating. The use of numerical gradients and the stochastic probability perturbation method makes the implementation quite easy, but both algorithms are very expensive computationally, which may limit the use of this procedure in practical settings.

In this work, we apply an adjoint model for the efficient calculation of gradients of the objective function with respect to the controls, which are then used

by gradient-based optimization algorithms such as sequential quadratic programming (SQP) [9] for optimization. For the model-updating procedure, we use Bayesian inversion theory and apply an efficient parameterization of the permeability field using the Karhunen–Loeve (K–L) expansion. This allows us to describe the uncertain parameter field (e.g., permeability), in terms of two-point statistics, using very few parameters. A key advantage of the K–L description is that these parameters can be continuously varied while maintaining the underlying geostatistical description. As a result, adjoint techniques can be applied for the history matching while preserving some degree of geological realism. This procedure is much faster than stochastic algorithms and, unlike standard gradient-based algorithms, implicitly honors the geology.

The use of adjoints for optimization and history matching has been the focus of active research for the past few decades. Ramirez and coworkers used it to optimize surfactant flooding [10], carbon dioxide flooding [11], and steam flooding [12]. Zakirov et al. [13] applied adjoint models to optimize production from a thin oil rim. Optimization of water flooding using adjoints has been studied by many researchers including Asheim [14], Virnovsky [15], Sudaryanto and Yortsos [16], and recently by Brouwer and Jansen [17]. The use of adjoints for history matching was pioneered by Chen et al. [18] and Chavent et al. [19], who applied it to single-phase problems. Since then, many other researchers have modified and improved the application of adjoint models for multiphase history matching including Wasserman et al. [20], Watson et al. [21], Wu et al. [22], Li et al. [23], Wu and Datta-Gupta [24], and Zhang et al. [25]. Gavalas et al. [26] introduced the use of an eigenfunction expansion for the efficient parameterization of reservoir properties, which was also used later by Oliver [27] and Reynolds et al. [28].

This article proceeds as follows. Sections 2 and 3 briefly describe the optimal control algorithm, and sections 4 and 5 describe the model-updating algorithm. These two elements are combined in a sequential manner to perform optimization for an uncertain reservoir description, as described in section 6. Two variants of the implementation of the model-updating algorithm within the closed loop are discussed. Next, the efficiency and applicability of this approach is demonstrated through a real-time dynamic water-flood optimization of a synthetic reservoir under production constraints and with an uncertain permeability field. The closed-loop optimization methodology is shown to provide a substantial improvement in NPV and sweep efficiency over the base case, and the results are quite close to those obtained with known geology.

2. Mathematical formulation of the problem

The production optimization problem under uncertainty as discussed above requires finding a sequence of control vectors u^n for $n = 0, 1, \ldots, N - 1$, where n is the

control step index and N is the total number of control steps, to maximize (or minimize) a performance measure $J(u^0, \ldots, u^{N-1})$. Our procedure for this optimization is discussed in detail by Sarma et al. [29], so our description here will be brief. The problem can be written as follows:

$$\max_{u^n} \left[J = \phi(x^N) + \sum_{n=0}^{N-1} L^n(x^{n+1}, u^n, m) \right] \forall n \in (0, \ldots, N-1)$$

subject to:

$$\begin{aligned}
& g^n\left(x^{n+1}, x^n, u^n, m\right) = 0 && \forall n \in (0, \ldots, N-1) \\
& x^0 = x_0 && \text{(Initial Condition)} \\
& c^n\left(x^{n+1}, u^n, m\right) \leq 0 && \forall n \in (0, \ldots, N-1) \\
& Au^n \leq b && \forall n \in (0, \ldots, N-1) \\
& LB \leq u^n \leq UB && \forall n \in (0, \ldots, N-1)
\end{aligned} \tag{1}$$

Here, x^n refers to the dynamic states of the system (pressures, saturations, compositions, etc.) and m refers to model parameters (permeability, porosity, etc.), which are assumed to be time invariant. Uncertainty enters the optimization due to uncertainty in m. The cost function J consists of two terms. The first term ϕ is a function only of the dynamic states of the last control step (e.g., abandonment cost). The second term is a summation over all control steps and consists of the kernel L^n, which is known as the Lagrangian in control literature [30]. Note that this definition is different from that of classical mechanics. Here it will involve the oil and water rates at each time step. The L^n term is treated fully implicitly because it involves quantities that are functions of well parameters.

The set of equations, g^n, together with the initial condition, defines the dynamic system. In the current application, g^n is the fully implicit reservoir simulation equations written for each grid block at each time step:

$$g^n\left(x^{n+1}, x^n, u^n, m\right) = \text{Accumulation terms} - \text{Flux terms} - \text{Well terms} \tag{2}$$

The last three equations of equation (1) define additional constraints for the controls – nonlinear constraints, linear constraints, and bounds. These equations constrain the controls directly, as opposed to the simulation equations (equation (2)) that constrain only the dynamic states. Note that the linear constraints are separately written from the nonlinear constraints as these and the bounds on controls are directly handled by the constrained optimization algorithm used (sequential quadratic programming [9]).

3. Optimal control with adjoint models

To perform the optimization component of the closed-loop (marked in blue in figure 1) with gradient-based methods, an efficient approach to calculate the gradients

of the cost function $J(u^0, \ldots, u^{N-1})$ with respect to controls u^n is required. The most efficient method of calculating these gradients entails the use of the adjoint equations. The adjoint equations are obtained from the necessary conditions of optimality of the problem defined by equation (1); these optimality conditions are given by the calculus of variations [30]. The key result is that the cost function of equation (1) constrained by the dynamical system can be written in terms of an augmented cost function:

$$J_A = \phi\left[x^N\right] + \sum_{n=0}^{N-1} L^n\left(x^{n+1}, u^n, m\right) + \lambda^{T0}\left(x_0 - x^0\right) + \sum_{n=0}^{N-1} \lambda^{T(n+1)} g^n\left(x^{n+1}, x^n, u^n, m\right) \tag{3}$$

Treatment of the other constraints is similar and is discussed in [29]. The vectors λ^n are Lagrange multipliers; one such multiplier is required for each constraint with which the cost function is augmented. For optimality of the original problem as well as the augmented cost function, the first variation of the augmented cost function must equal zero [30]. The first variation of J_A is given by:

$$\begin{aligned}\delta J_A = &\left[\left.\frac{\partial \phi}{\partial x}\right|_{x=x^N} + \frac{\partial L^{N-1}}{\partial x^N} + \lambda^{TN}\frac{\partial g^{N-1}}{\partial x^N}\right]\delta x^N + \sum_{n=0}^{N-1}[g^n]\delta\lambda^{T(n+1)} + \left(x_0 - x^0\right)\delta\lambda^{T0} \\ &+ \sum_{n=1}^{N-1}\left[\frac{\partial L^{n-1}}{\partial x^n} + \lambda^{T(n+1)}\frac{\partial g^n}{\partial x^n} + \lambda^{Tn}\frac{\partial g^{n-1}}{\partial x^n}\right]\delta x^n + \sum_{n=0}^{N-1}\left[\frac{\partial L^n}{\partial u^n} + \lambda^{T(n+1)}\frac{\partial g^n}{\partial u^n}\right]\delta u^n\end{aligned} \tag{4}$$

Note that variation of m does not appear in equation (4) as m is independent of u^n. Since the variations of x^n, u^n, and λ^n are independent of one another, each of these terms must vanish for optimality [30]. The $g^n\delta\lambda^{T(n+1)}$ and $(x_0 - x^0)\delta\lambda^{T0}$ terms are zero by definition. The terms involving δx^n will vanish if λ^n satisfies:

$$\begin{aligned}\lambda^{Tn} &= -\left[\frac{\partial L^{n-1}}{\partial x^n} + \lambda^{T(n+1)}\frac{\partial g^n}{\partial x^n}\right]\left[\frac{\partial g^{n-1}}{\partial x^n}\right]^{-1} \quad \forall n = 1, \ldots, N-1 \\ \lambda^{TN} &= -\left[\left.\frac{\partial \phi}{\partial x}\right|_{x=x^N} + \frac{\partial L^{N-1}}{\partial x^N}\right]\left[\frac{\partial g^{N-1}}{\partial x^N}\right]^{-1} \quad \text{(Final Condition)}\end{aligned} \tag{5}$$

Equation (5) defines the adjoint model. Because the Lagrange multipliers λ^n depend on λ^{n+1}, the adjoint model is solved backwards in time, with the second equation above providing λ at the last time step (i.e., the initial condition for the backward integration). Equation (4) can now be written as:

$$\delta J_A = \sum_{n=0}^{N-1}\left[\frac{\partial L^n}{\partial u^n} + \lambda^{T(n+1)}\frac{\partial g^n}{\partial u^n}\right]\delta u^n \tag{6}$$

Thus the gradients of the cost function with respect to the controls are given as:

$$\frac{dJ}{du^n} = \frac{dJ_A}{du^n} = \left[\frac{\partial L^n}{\partial u^n} + \lambda^{T(n+1)} \frac{\partial g^n}{\partial u^n}\right] \quad \forall n \in (0, \ldots, N-1) \tag{7}$$

These gradients can be used with any gradient-based algorithm to determine the new search direction and thereby the new u^n. The basic steps required for gradient-based optimization with adjoints, as given in [29], are as follows:

1. Solve the forward model equations for all time steps with given initial condition and initial control strategy. Store the dynamic states at each time step.
2. Calculate the cost function with results of the forward simulation.
3. Solve the adjoint model equations using the stored dynamic states to calculate the Lagrange multipliers with equation (5).
4. Use the Lagrange multipliers to calculate the gradients using equation (7) for all control steps.
5. Use these gradients with any gradient-based optimization algorithm to choose new search direction and control strategy.
6. Repeat process until optimum is achieved, that is, all gradients are sufficiently close to zero.

This is a very efficient procedure, as the time required to solve the adjoint model (and to calculate all of the required gradients) is about the same as that needed for the forward simulation. For further algorithmic details on our implementation of the adjoint model within the context of a fully implicit general-purpose reservoir simulator, and for a description of the treatment of nonlinear constraints, refer to [29].

4. Model updating as a minimization problem

A number of techniques are available for the history-matching problem. Gradient-based procedures are in general very efficient, but standard implementations suffer from two limitations. First, they tend to find local, rather than global, minima. Although this is the case to some extent with all history-matching algorithms, stochastic optimization techniques introduce a random component to sample the parameter space more broadly. The second limitation inherent in standard gradient-based techniques is that geological constraints are not preserved. This occurs because, during the optimization, geostatistical correlations between model parameters are not maintained.

The technique applied here circumvents this latter difficulty by introducing an efficient parameterization of the permeability field in terms of the Karhunen–Loeve

expansion (the K–L expansion, described in more detail below, is essentially an eigenfunction expansion) [26–28]. Because the parameters appearing in the K–L expansion are uncorrelated, any set of these parameters provides a permeability field that honors the underlying two-point geostatistics. Thus, these parameters can be varied in any way to achieve a history match. The technique is much more efficient than stochastic search procedures and has the additional advantage that much of the adjoint code developed for the production optimization problem can also be applied with some modifications to the history-matching problem.

The model-updating component of the closed loop is a problem of inversion of production data (well pressures and flow rates) in order to determine reliable estimates of uncertain model parameters (porosity and permeability). Within the context of Bayesian inverse modeling, the solution to the general inverse problem consists of combining all prior information as given by the prior probability density of the observed data d, given by $\rho_D(d)$, the prior probability density of the model parameters m, given by $\rho_M(m)$, and the forward model $d = f(m)$ to determine the posterior probability density of the model parameters $\sigma_M(m)$ given by the following general equation [31]:

$$\sigma_M(m) = k\rho_M(m)\rho_D(f(m)) \tag{8}$$

where k is a constant. The most general solution for solving any nonlinear inverse problem involves determining the entire probability distribution $\sigma_M(m)$, which requires an extensive exploration of the model space, usually accomplished using random search techniques such as a Monte Carlo method [31].

For the case of history matching, however, solving the forward model $d = f(m)$ is usually very time-consuming, and in practical cases a single evaluation can take several hours of computation. Therefore we must often be satisfied with the determination of the maximum likelihood and a reasonable estimate of the dispersion of the distribution around it. This is generally accomplished through least-squares techniques, which is a special case of equation (8), when both the prior probability densities $\rho_M(m)$ and $\rho_D(d)$ are Gaussian. Under these assumptions, the model-updating problem reduces to the minimization of the following misfit function, where C_D and C_M are the data and parameter prior covariance matrices [31]:

$$S(m) = (f(m) - d_{obs})^T C_D^{-1}(f(m) - d_{obs}) + (m - m_{prior})^T C_M^{-1}(m - m_{prior}) \tag{9}$$

In the general problem of model updating, the forward model $d = f(m)$ (simulation equations and outputs) is not only a function of the model parameters m, but is also a function of the dynamic states x (grid pressures, saturations, etc.) and a set of controls u (well rates, bottom hole pressures, etc.), that is, $d^n = f(x^{n+1}, u^n, m)$, where n is the time-step index (m is assumed to be time-invariant). The dynamic states x are

functions of both m and u. Thus the mathematical formulation of the general model-updating problem is as follows:

$$\min_m \left[S = \left(m - m_{prior}\right)^T C_M^{-1} \left(m - m_{prior}\right) + \sum_{n=0}^{N-1} L^n\left(x^{n+1}, u^n, m\right) \right] \forall n \in (0, \ldots, N-1)$$

subject to:

$$\begin{aligned} & g^n\left(x^{n+1}, x^n, u^n, m\right) = 0 \qquad \forall n \in (0, \ldots, N-1) \\ & x^0 = x_0 \qquad\qquad\qquad\qquad \text{(Initial Condition)} \\ & m \in \text{Geologically Consistent Realizations} \end{aligned} \tag{10}$$

The Lagrangian $L^n(x^{n+1}, u^n, m)$ has the following form for the history-matching problem (assuming that measurement uncertainties are independent):

$$L^n\left(x^{n+1}, u^n, m\right) = \sum_{i=1}^{N_w} \left\{ \frac{f_i^n\left(x^{n+1}, u^n, m\right) - d_{obs_i}^n}{\sigma_i^n} \right\}^2 \tag{11}$$

Here σ_i^n is standard deviation of the measured data and N_w is number of wells. The set of equations $g^n(x^{n+1}, x^n, u^n, m) = 0$, together with the initial condition $x^0 = x_0$, refers to the reservoir simulation equations (forward model) that constrain the dynamic states x. The geological constraints (last set of constraints in equation (10)) are required because production data on its own is not fully constraining. Even with these geological constraints the system is still not fully constrained, but the use of these constraints guarantees that the resulting m will be consistent with the geostatistical description.

5. Bi-orthogonal expansions and adjoints for updating

As noted before, standard gradient-based algorithms will not maintain the necessary geological constraints. As a result, although the objective function might be reduced by a large amount, the final m may not be geologically realistic, which may in turn result in poor predictions. By introducing the K–L expansion of the random parameter field m, the problem defined in equation (10) is transformed such that the geological constraints (as defined by the covariance matrix of m) are implicitly honored. In addition, the number of parameters defining m is decreased significantly, resulting in a greater reduction of the uncertainty envelope compared to the direct solution of the original problem [27, 28].

The Karhunen–Loeve expansion is a very powerful tool for representing stationary and nonstationary processes with explicitly known covariance functions. Any random field or process can be represented as a series expansion involving a complete set of deterministic functions with corresponding random coefficients [32]. This method provides a second-moment characterization in terms of random variables

and deterministic functions. The use of K–L expansion with orthogonal deterministic basis functions and uncorrelated random coefficients has generated interest because of its biorthogonality property, that is, both the deterministic basis functions (eigenfunctions) and the corresponding random coefficients are orthogonal. This allows for the optimal encapsulation of the information contained in the random process into a set of discrete uncorrelated random variables. For a random field $m(x, \theta)$ with a finite variance and a mean $\overline{m}(x)$, the K–L expansion in continuous form is given as [33]:

$$m(x,\theta) = \overline{m}(x) + \sum_{i=1}^{\infty} \sqrt{\lambda_i} f_i(x) \xi_i(\theta) \tag{12}$$

Here, x is the spatial (or temporal) variable, θ is a random event, $\xi_i(\theta)$ is a set of uncorrelated random variables, and λ_i and $f_i(x)$ are the eigenvalues and eigenfunctions of the covariance function $C(x_1, x_2)$ of $m(x, \theta)$. By definition, $C(x_1, x_2)$ is bounded, symmetric, and positive definite. Following Mercer's theorem [32], C has the following spectral or eigen decomposition:

$$C(x_1,x_2) = \sum_{i=1}^{\infty} \lambda_i f_i(x_1) f_i(x_2) \tag{13}$$

Because reservoir simulation models are defined on discrete grids, we are more interested in the discrete form of the K–L expansion. The truncated K–L expansion of the correlated (geologically constrained) random variables m is given as:

$$[m]_{H,1} = [\Phi]_{H,K} [\Sigma]_{K,K} [\xi]_{K,1} + [\overline{m}]_{H,1} \tag{14}$$

Here, Φ is the matrix of the eigenvectors corresponding to the K largest eigenvalues of the covariance matrix C_M, Σ is a diagonal matrix consisting of the K largest standard deviations (square roots of eigenvalues), ξ is a vector of uncorrelated random variables with zero mean and unit variance (dimension K), and $\overline{m}$ is the expected value of m. In practice, $K << H$, where H is the dimension of m (e.g., if the geology is characterized by porosity and isotropic permeability, $H = 2N_b$, where N_b is the total number of grid blocks in the problem). Thus m is represented by a much smaller set of parameters ξ. Using this expansion for m, the proposed formulation of the model-updating problem is as follows:

$$\begin{aligned} &\min_{\xi} \left[S = \{m(\xi) - m_{prior}(\xi)\}^T C_M^{-1} \{m(\xi) - m_{prior}(\xi)\} + \sum_{n=0}^{N-1} L^n(x^{n+1}, u^n, m(\xi)) \right] \\ &\qquad \forall n \in (0, ..., N-1) \\ &\text{subject to:} \\ &g^n(x^{n+1}, x^n, u^n, m(\xi)) = 0 \qquad \forall n \in (0, \ldots, N-1) \\ &x^0 = x_0 \qquad \text{(Initial Condition)} \end{aligned} \tag{15}$$

The problem is thus formulated with ξ as the unknown parameters. Since the components of ξ are uncorrelated, the optimization (minimization) algorithm is free to

modify ξ in any manner; i.e., whatever the values of ξ, the set of m obtained from them using equation (14) will always be correlated according to the correlation structure of the covariance matrix. Thus any gradient-based algorithm can be used to accomplish the minimization using ξ as the unknowns while at the same time honoring the geological constraints for m.

As in the optimization problem, an adjoint model is used to calculate the gradients of the objective function S with respect to the parameters ξ. Using the same approach as in the production optimization problem (i.e., adjoining the dynamic system to the objective function), the adjoint model is derived as:

$$\begin{aligned} \lambda^{Tn} &= -\left[\frac{\partial L^{n-1}}{\partial x^n} + \lambda^{T(n+1)}\frac{\partial g^n}{\partial x^n}\right]\left[\frac{\partial g^{n-1}}{\partial x^n}\right]^{-1} \quad \forall n = 1, \ldots, N-1 \\ \lambda^{TN} &= -\left[\frac{\partial L^{N-1}}{\partial x^N}\right]\left[\frac{\partial g^{N-1}}{\partial x^N}\right]^{-1} \quad \text{(Final Condition)} \end{aligned} \tag{16}$$

After λ is calculated using the adjoint model, the derivative of S with respect to m is calculated as:

$$\frac{dS}{dm} = \sum_{n=0}^{N-1}\left\{\frac{\partial L^n}{\partial m} + \lambda^{T(n+1)}\frac{\partial g^n}{\partial m}\right\} + \left\{2C_M^{-1}\left(m - m_{prior}\right)\right\}^T \tag{17}$$

Equation (17) can be used to calculate the gradient of S with respect to ξ using the chain rule and equation (12):

$$\frac{dS}{d\xi} = \frac{dS}{dm}\frac{dm}{d\xi} = \left[\sum_{n=0}^{N-1}\left\{\frac{\partial L^n}{\partial m} + \lambda^{T(n+1)}\frac{\partial g^n}{\partial m}\right\} + \left\{2C_M^{-1}\left(m - m_{prior}\right)\right\}^T\right][\Phi][\Sigma] \tag{18}$$

This completes the description of the history-matching procedure. Many of the main components of this adjoint, such as $\partial g^{n-1}/\partial x^n$, are already calculated and stored for the production optimization problem, and can thus be easily reused, leading to added efficiency. We note that the use of the Jacobian from the fully implicit forward problem in the history matching algorithm was previously introduced by Li et al. [23].

6. Implementation of the closed loop

The formulation of the closed loop (without uncertainty propagation) can be implemented very efficiently with the components discussed above. The main steps required to complete the loop are as follows:

1. From the prior model of the uncertain but correlated parameter field, calculate the covariance matrix, either numerically or analytically. Note that the covariance model may be nonstationary.

2. Perform K–L expansion to determine the eigenvectors and eigenvalues of the covariance matrix. Retain only the largest eigen-pairs; the number to be retained can be determined from the percentage of the total energy contained in the eigen-pairs.
3. Perform optimization from control step k to N_t, (total control steps) starting with $k = 1$, that is, the first control step, using the current maximum likelihood estimate of the parameter field m.
4. Apply the optimized trajectory of the controls on the "true" reservoir from control step k to $k + 1$, and record the reservoir response for this time period. This provides the "data" to be used for history matching.
5. Perform model updating to assimilate new data. Updating can be performed from control step 1 to the step $k + 1$, that is, assimilate new data and reassimilate earlier data, or from step k to $k + 1$, that is, only assimilate new data.
6. Perform optimization step 3 for the next control step, that is, $k = k + 1$, with the new maximum likelihood estimate of the parameter field obtained from step 5. Repeat steps 3 to 6 until $k = N_t$.

Some of the above steps require further elaboration. If the prior model of the parameter field is multi-Gaussian, the covariance matrix can be calculated analytically. In general, especially if the prior model is obtained from multi-point geostatistics, the covariance matrix must be calculated numerically from a large number of realizations of the prior model. The covariance matrix will be nonstationary if prior conditioning data such as hard data are present. The Karhunen–Loeve expansion can be performed using singular value decomposition (SVD). However, since the standard implementation of SVD is a very expensive process, special techniques such as the Lanczos algorithm [34] for determining only the dominant eigen-pairs may be used.

For each optimization step, the optimization process must be performed to the last control step N_t, even though only the trajectory from step k to $k + 1$ is actually applied on the "true" reservoir. This is because we are interested in long-term optimization, and future events (beyond step $k + 1$) can have significant impact on the optimal trajectory from step k to $k + 1$. However, if the maximum likelihood estimate of the parameter field does not change much from one update to the next, the optimal trajectory obtained in the next optimization loop should not be very different from the last optimization, and therefore, techniques such as neighboring optimal control [30] might be used for added efficiency.

The two methods to perform data assimilation discussed in step 5 constitute the two variants of the model-updating process considered here. The traditional approach to history matching is to use all existing data at any given time to execute the updating process, even though some of that data may have been previously assimilated. This is required to maintain consistency (history match) with all existing data if the standard form of the least square error is used as the objective function (without the prior term as in equation (15)).

The updating process can, however, be made much more efficient by performing the update only from step k to $k + 1$, that is, only assimilating new data. Consistency

with previously assimilated data can be maintained approximately by using the prior term in the objective function (equation (15)), with each new updating step starting with the maximum likelihood estimate from the previous step as m_{prior} and the posterior covariance matrix from the previous step as the new prior covariance C_M. The covariance changes from one step to the next because the dynamic data being assimilated introduces correlations into ξ (independent initially by construction) after each model update. As a result, at each model-updating step, a new K–L expansion must be performed on the small covariance matrix of ξ (designated C_ξ) but not on C_M (C_ξ is of dimension 20 $\times$ 20 in the example below, as opposed to 2,025 $\times$ 2,025, the size of C_M). This K–L expansion of the now correlated ξ then replaces the vector ξ in equation (14), thus giving a new set of independent ξ, used for updating the next control step.

Because C_ξ generally reduces from step to step as new data are assimilated, the m associated with different choices of ξ will look increasingly similar to the most recent m_{prior}. Using this approach, previously assimilated data, although not directly assimilated from step k to $k + 1$, appear indirectly through m_{prior} and C_ξ. Further, as we proceed from one control step to the next, since C_ξ reduces (i.e., the variance of ξ reduces), the weight of the prior term in the objective function increases, implying that deviation from m_{prior} becomes more difficult as time proceeds. This can be helpful in alleviating problems such as those observed in [4], where late-time updates became problematic, presumably due to the assimilation of noise.

The total time required to perform one cycle of the closed loop at control step k can be quantified in terms of the total number of simulations required. One iteration of the optimization algorithm requires an equivalent of two simulations (from $k = k$ to N_t) to calculate the gradients (if constraints are implemented internally) and 1–4 simulations (from $k = k$ to N_t) to calculate the step size in the search direction (using sequential quadratic programming). Typically, 4–6 iterations result in substantial improvements in the objective function. Similarly, for the model-updating component, using the first approach, an equivalent of two simulations (from $k = 1$ to k) is required to calculate the gradients and 1–4 simulations (from $k = 1$ to k) to calculate the step size in the search direction. Using the second approach for model updating, the simulation length is reduced to one control step. Usually, about 5–10 iterations result in convergence. Thus, if we update the reservoir model and controls 10 times over the course of the simulated production, the equivalent of about 300 (120 for optimization + 180 for model updating) complete simulations (from $k = 0$ to N_t) would be required under the first approach, compared to about 155 (120 for optimization + 35 for model updating) complete simulations using the second approach.

7. Case study – dynamic waterflooding

The closed-loop approach discussed above is now applied to an idealized example case somewhat similar to that used by Brouwer et al. [4]. This case was

chosen primarily because it effectively demonstrates the applicability of adjoint-based optimization to smart well control and because it illustrates that the model-updating approach can be successfully used with realizations based on multipoint (as opposed to two-point) geostatistics. In addition, this example allows us to qualitatively compare our model-updating approach to Kalman filters as used by Brouwer et al. [4].

The schematic of the reservoir and well configuration is shown in figure 2. The model consists of one horizontal "smart" water injector and one horizontal "smart" producer, each having 45 controllable segments. The reservoir covers an area of 450 $\times$ 450 m^2 and has a thickness of 10 m and is modeled by a 45 $\times$ 45 $\times$ 1 horizontal 2D grid. The fluid system is essentially an incompressible two-phase unit mobility oil–water system, with zero connate water saturation and zero residual oil saturation.

In order to apply the closed-loop approach, one or more of the reservoir properties must be unknown. For this example, permeability is assumed to be unknown and will be updated by assimilating production data. Further, it is assumed that we have some prior knowledge of the reservoir, which informs us that the reservoir is a fluvial channelized reservoir as depicted by the training image [35] shown in figure 3, with the channel sand permeability being about 10 Darcy and the background sand permeability about 500 mDarcy. The contrast in permeability between the high-permeability sand and the background reservoir is about a factor of 20, and it is this heterogeneity that makes the optimization results interesting.

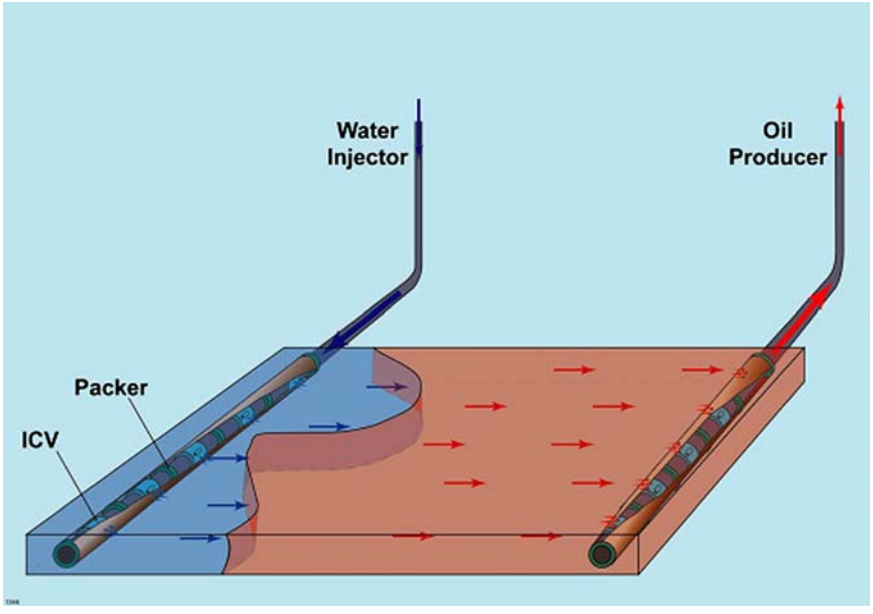

Figure 2. Schematic of reservoir and wells for example case (from Brouwer and Jansen [17]).

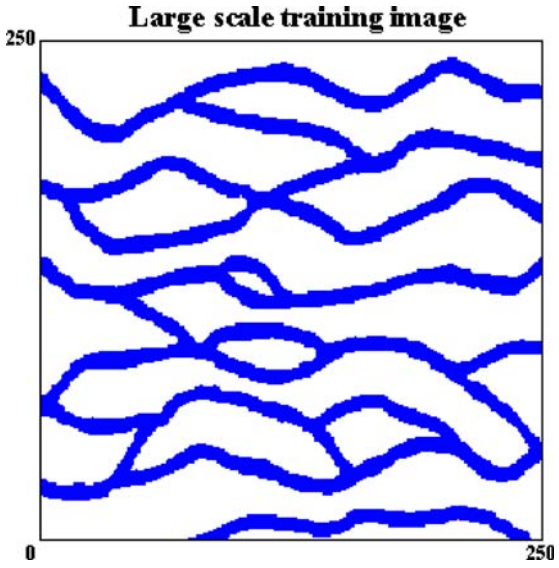

Figure 3. Training image used to create the original realizations (from Strebelle [35]).

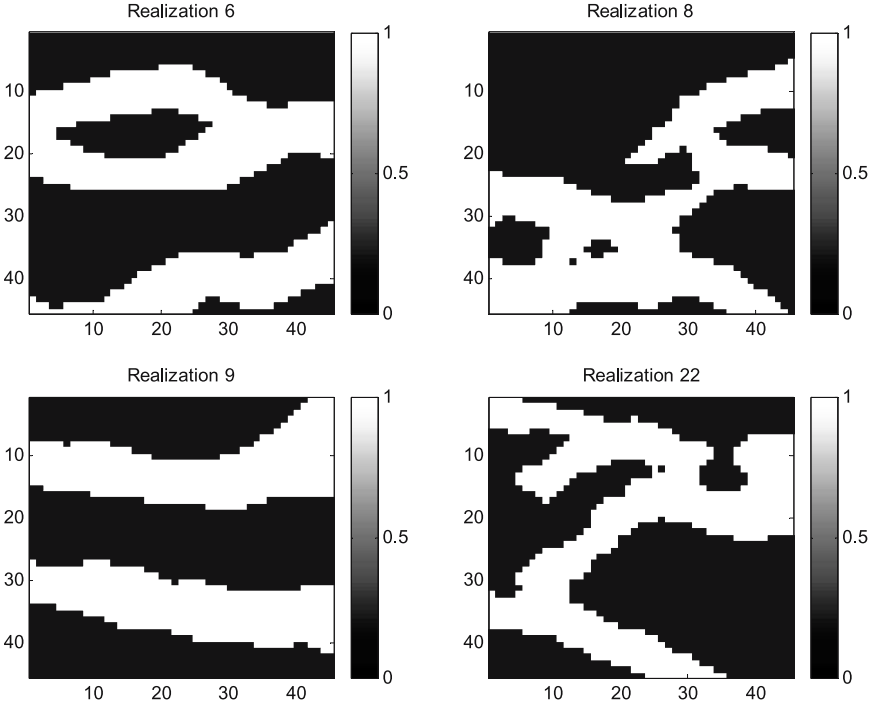

Figure 4. Some of the realizations created with *snesim* [35]; realization 9 is assumed to be the "true" realization for case 1 and realization 8 is the initial guess.

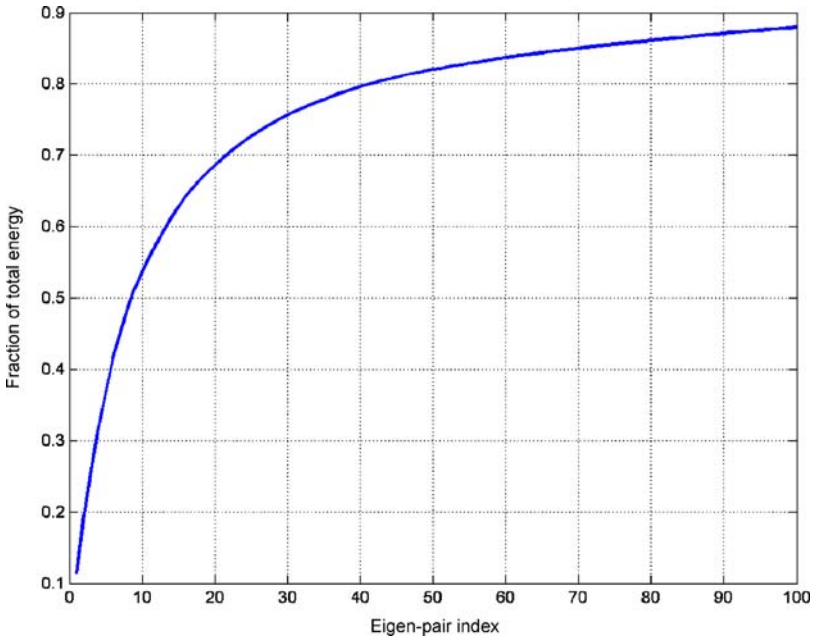

Figure 5. Energy retained in the first 100 eigen-pairs.

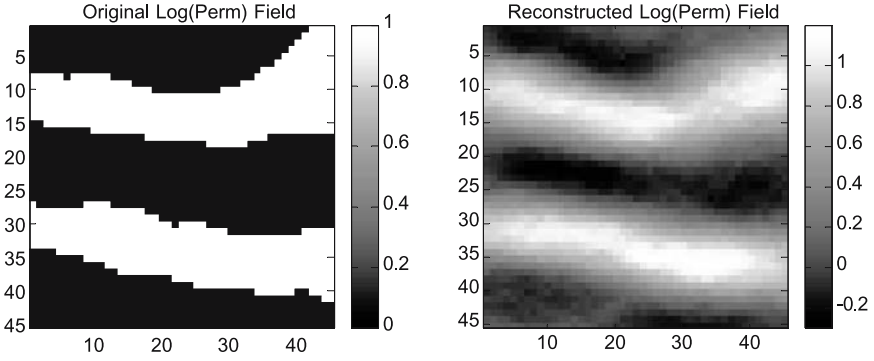

Figure 6. Reconstruction of "true" realization with 20 eigen-pairs.

Figure 4 shows some unconditioned realizations of the permeability field generated using the *snesim* software [35] with the training image of figure 3. To validate our closed-loop approach, a "true" realization is required, against which the optimization and model updating results can be compared. Realization 9 from figure 4 is taken to be the "true'' reservoir. Note that although we are using unconditioned realizations for this example, realizations conditioned to hard data can be used just as easily with this approach. In the absence of any other data, all realizations obtained from *snesim* are equiprobable; thus any realization could be chosen as an initial guess.

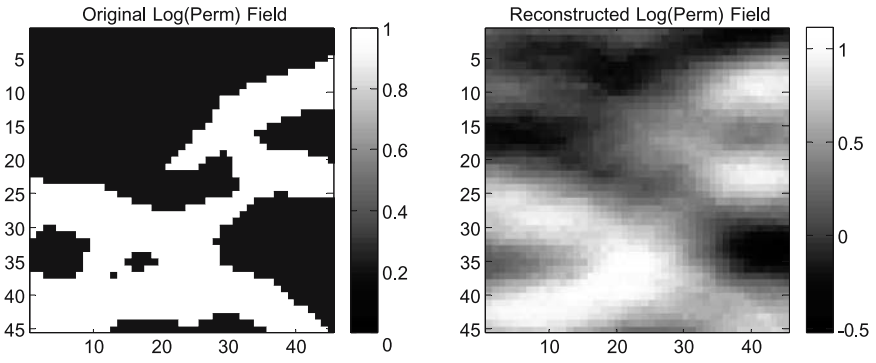

Figure 7. Reconstruction of initial realization with 20 eigen-pairs.

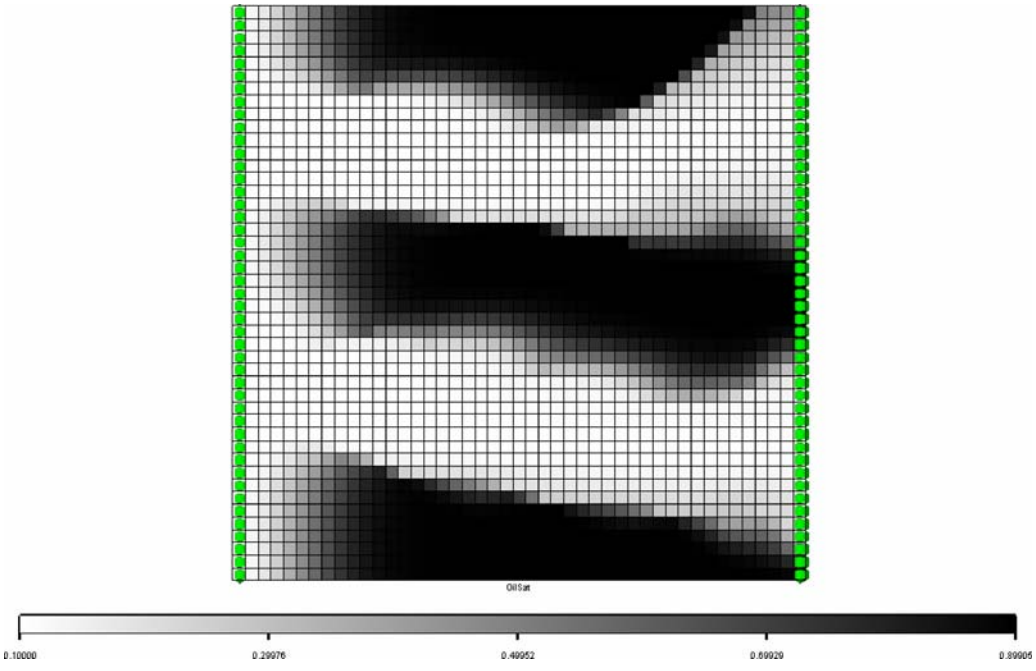

Figure 8. Final oil saturations after one PV injection for reference case with "true" realization.

We choose realization 8 to be the initial guess. Note that the connectivity and the location of the channels are quite different in these two realizations, and therefore the nature of the production data would also be very different, particularly in terms of important features such as breakthrough times.

Karhunen–Loeve expansion is performed using the covariance matrix created from 1,000 initial realizations. The energy retained in the eigen-pairs is plotted in figure 5. We observe that most of the energy is associated with the first few eigen-pairs. Figures 6 and 7 show the reconstructions of the true and initial permeability

fields using 20 eigen-pairs. It is clear that although the long correlation structures (low frequencies) are essentially preserved, the smaller correlation structures (high frequencies) are lost, which results in a smoothing effect. Although this smoothing results in an approximation of the actual multipoint geostatistics, it is beneficial in that it provides smoother gradients, which in turn leads to better convergence behavior of the minimization algorithm. For the purpose of model updating, we chose to retain only 20 eigen-pairs; this corresponds to about 70% of the total energy.

For purposes of optimization, the injector segments are placed under rate control, and the producer segments are under BHP control. There is a total injection constraint of 2,700 bbl/day (STBD); thus the optimization essentially results in a redistribution of this water among the injection segments. There are also bounds on the minimum and maximum rates allowed per segment, as well as bounds on the BHP of the producers, which could, for example, correspond to bubble point pressures or fracture pressures. The model is produced until exactly one pore volume of water is injected, which corresponds to around 950 days of injection. This time period is divided into seven control steps of 30, 60, 100, 190, 190, 190, and 190 days. Thus the total number of controls is equal to $(45 + 45) \times 7 = 630$. All constraints in this problem are linear with respect to the controls. These seven control steps also correspond to the model-updating steps. The injection BHP and producer water and oil rates from the "true" model are used as data to update the permeability field. Since these measurements are

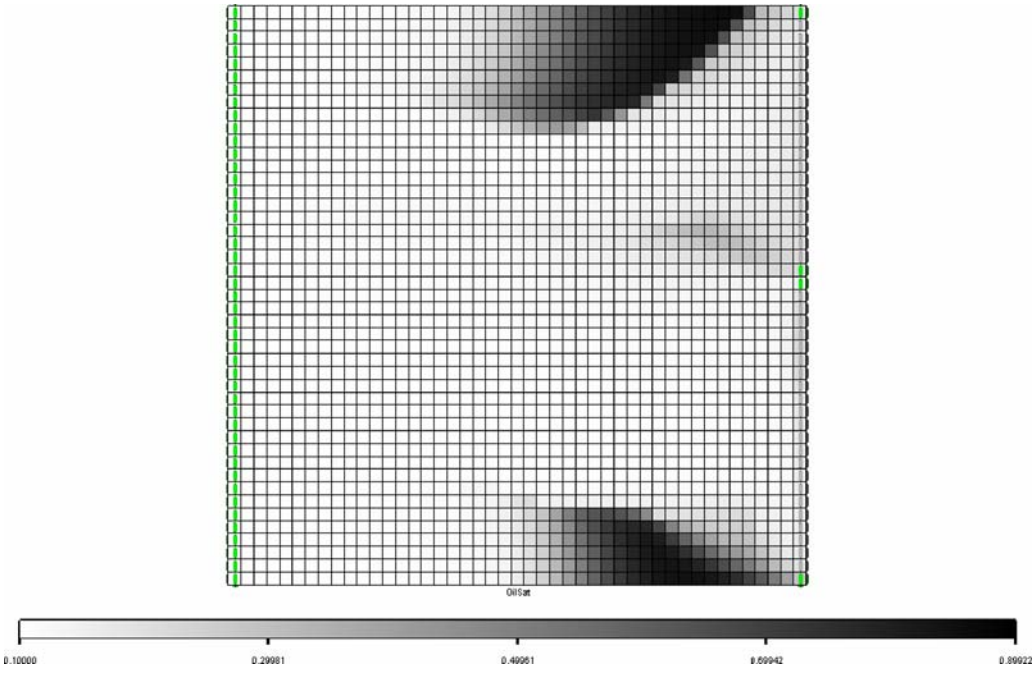

Figure 9. Final oil saturations after one PV injection for optimization with "true" realization.

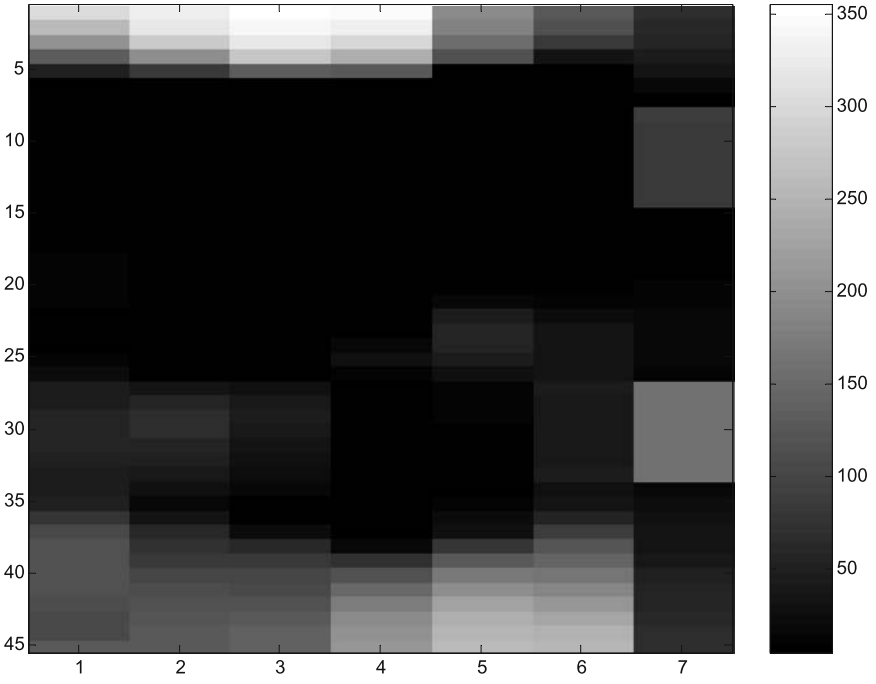

Figure 10. Injection rate variation with time for optimization with "true" realization.

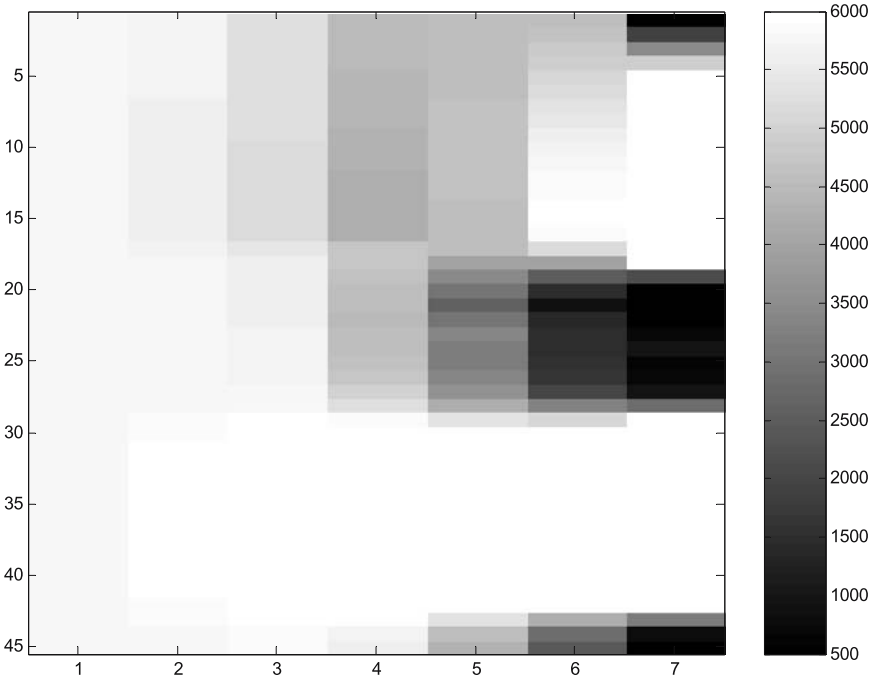

Figure 11. Producer BHP variation with time for optimization with "true" realization.

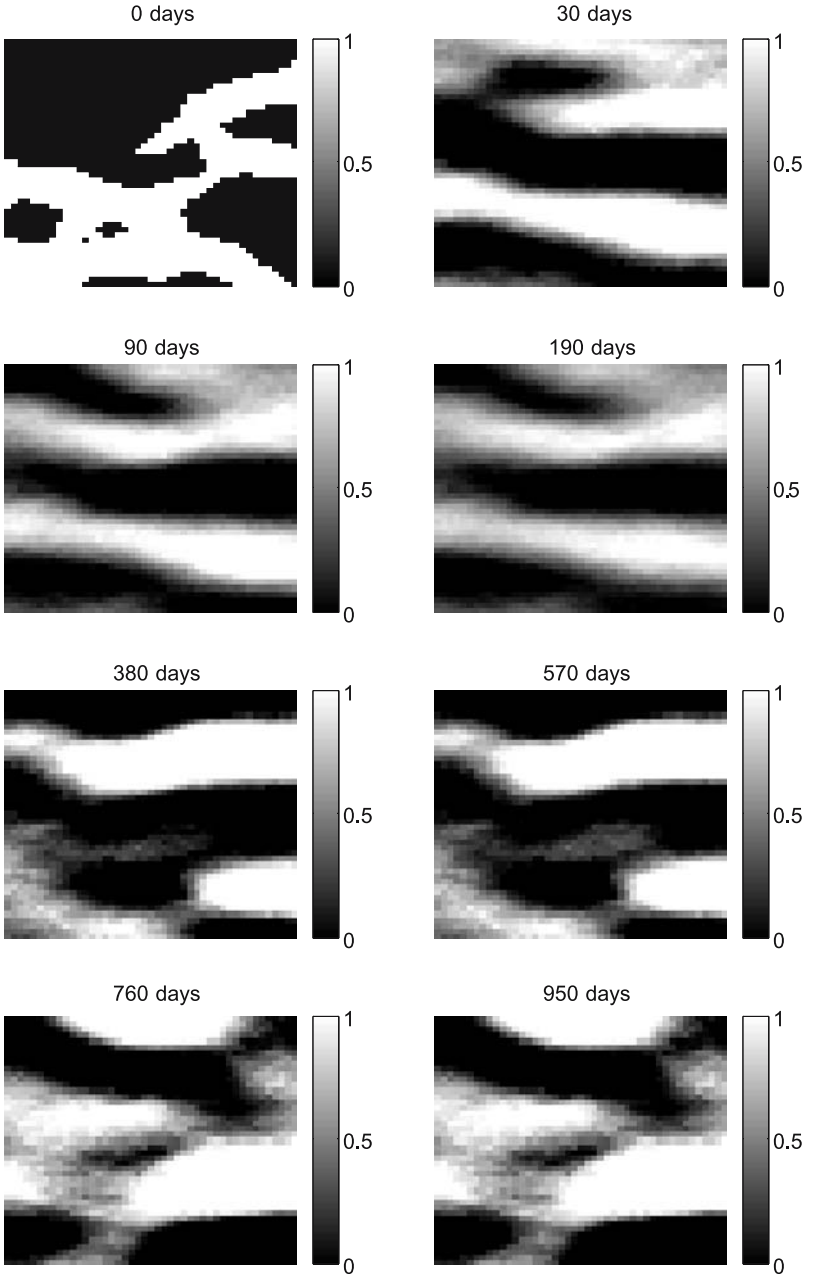

Figure 12. Permeability field updates with model updating performed using all available data and without prior term in objective.

synthetic, they are noise-free, although in reality these measurements would also contain noise, which can be accounted for using C_D.

In order to understand the benefit of any optimization process, it is usual to compare the optimization results against a base or reference case. In the case of production optimization, such a base case would be a reasonable production strategy that an engineer might devise given a simulation model and a set of constraints. For the purpose of this case study, the base case is a constant rate/constant BHP production strategy. The 2,700 STBD of injection water is distributed among the 45 injection segments according to their *kh*, which corresponds to an uncontrolled case. The producer BHP are set in such a way that a balanced injection–production is obtained, meaning that total liquid injection is equal to total liquid production.

The objective of the optimization process is to maximize net present value (NPV), defined by the equation below:

$$L^n = \frac{\Delta t^n}{(1+\alpha)^{t^n}} \left[\sum_{j=1}^{N_p} \left[P_{op} q^n_{o,j} - C_{wp} q^n_{wp,j} \right] - \sum_{j=1}^{N_I} C_{wi} q^n_{wi,j} \right] \tag{19}$$

Here Δt is the length of the control step, P_{op} is the oil price/bbl, q_o is the oil production rate, C_{wp} is the water production costs/bbl, q_{wp} is the water production rate, C_{wi} is the

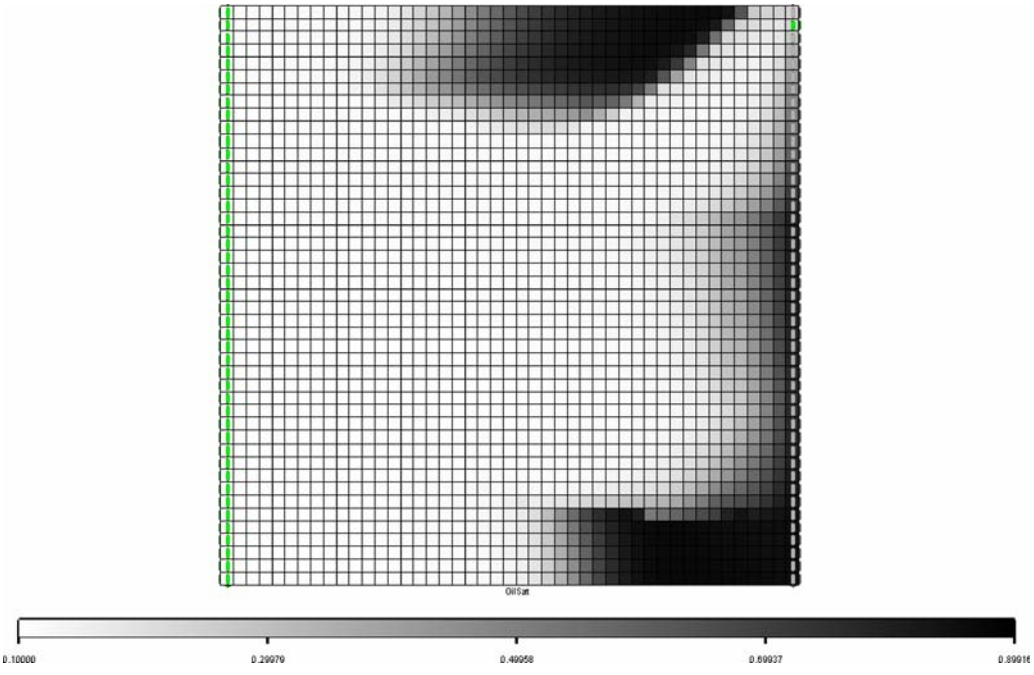

Figure 13. Final oil saturations after one PV injection for optimization with model updating using first approach.

water injection cost/bbl, q_{wi} is the water injection rate, N_p is the number of producers, N_I is the number of injectors, and α is the discounting factor. The NPV discounting factor α is set to zero, meaning that the effect of discounting is neglected. Thus, maximizing NPV is essentially maximizing cumulative oil production and minimizing cumulative water production. The oil price is conservatively set at 80 \$/m^3, water injection costs at 0 \$/m^3, and water production costs at 20 \$/m^3. It should be noted that it is relatively easy to vary these cost/prices with time or to implement uncertainty models for them.

The optimization process is first demonstrated assuming that the "true" permeability field is known, and to realize the benefit of the process, it is compared against the reference case, also evaluated using the "true" permeability. This constitutes what is known as an "open-loop" optimization. Starting from 100% oil saturation throughout the reservoir, figures 8 and 9 show the final oil saturations for the uncontrolled and the optimized case after exactly 1 PV of water has been injected. It is clear that the optimization leads to a substantial improvement in the sweep efficiency, leading to the increase in NPV of almost 100%.

The reasons behind the better sweep in the optimized case can be readily explained by analyzing the optimized trajectories of the controls – rates/BHP of the injectors and producers – as seen in figures 10 and 11. The y-axis of figure 10

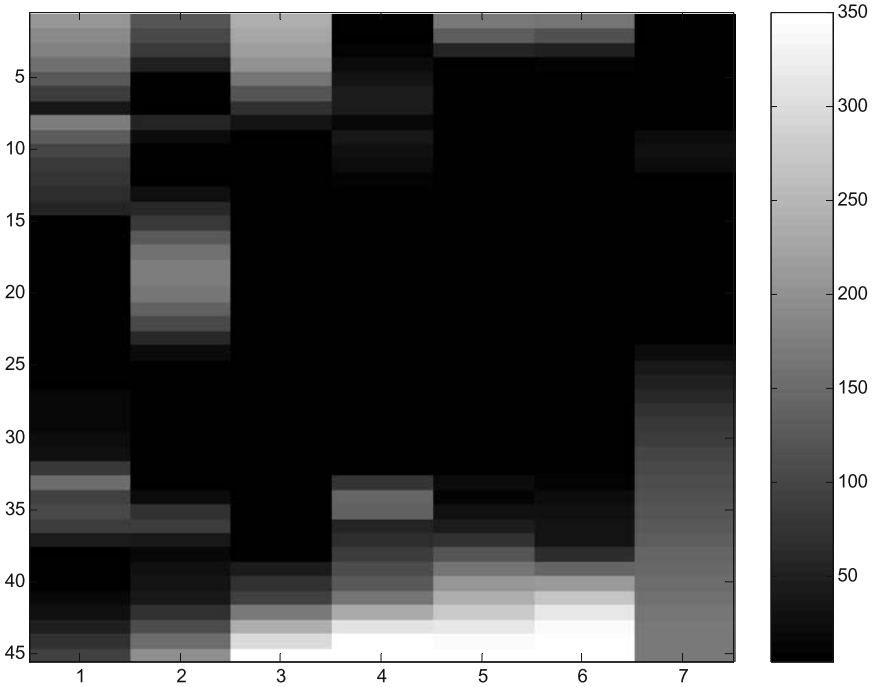

Figure 14. Injection rate variation with time for optimization with model updating using first approach.

corresponds to 45 injector segments and the x-axis corresponds to the seven control steps. The scale corresponds to injection rates of the segments, with black being the lowest rates (almost closed) and white being the highest rates (fully open). It is clear that the injector segments completed in or near the high-permeability streaks are nearly shut for most of the time, as they would otherwise force water to move very rapidly toward the producers, resulting in early breakthrough and thus poor sweep. Furthermore, injector segments at the edges of the reservoir are almost fully open, which forces the water front away from the high-permeability streaks to move laterally, resulting in an almost 100% sweep of these regions. In figure 11, the scale corresponds to the BHP of the producer segments, and we again observe that the producer segments completed in or near the high-permeability streaks are shut most of the time. Also, the producer segments between the streaks open more toward the later control steps, thus moving the water present in the streaks toward this region, which in turn leads to a better sweep.

The open-loop approach discussed above required that the permeability field (and other reservoir properties) be completely known. However, in reality, we never have complete knowledge of the reservoir, and thus the closed-loop approach must be used. The results of the open-loop approach can usually be thought of as the best possible results that can be achieved by any closed-loop approach, naturally under the assumption that the same search algorithms and the same initial starting point for the

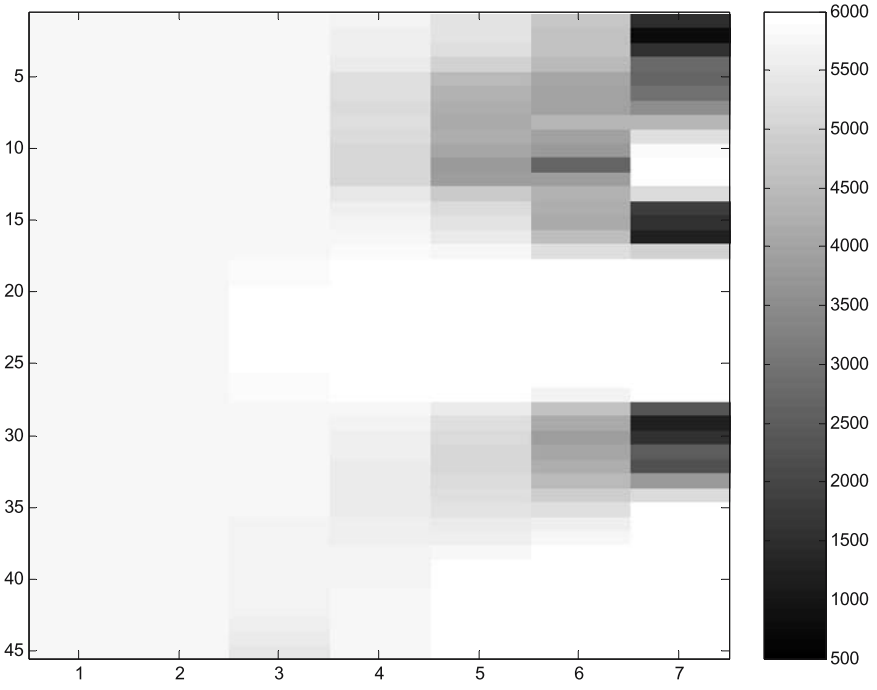

Figure 15. Producer BHP variation with time for optimization with model updating using first approach.

controls is used. It can thus be used as a benchmark against which closed-loop algorithms can be compared. In the following set of results, we apply the closed-loop procedure.

Figure 12 shows the permeability field updates obtained using the first model-updating approach, but without the prior term in the objective function. Comparing to the "true" realization (realization 9 in figure 4), it is clear that the correct channel locations and connectivity are well approximated even after the first update at 30 days. However, the model appears to deteriorate somewhat at later times, and this may be due to overfitting, which is possible due to the absence of the prior term. To elaborate, the prior term indirectly takes into account previously assimilated data by not allowing the solution to move too far from the previous prior estimate according to the weight of the prior term. Since the previous prior estimate was a result of assimilation of previous data, the amount of data "available" for the history match is greater (indirectly) when the prior term is present, although the number of parameters ξ is the same for both cases. Figure 13 shows the final oil saturations obtained using this closed-loop approach. Comparing this to figures 8 and 9, we see that the sweep obtained is greatly improved over the uncontrolled case, and is almost as good as that using the open-loop approach. Comparing figures 14 and 15 to figures 10 and 11, it is

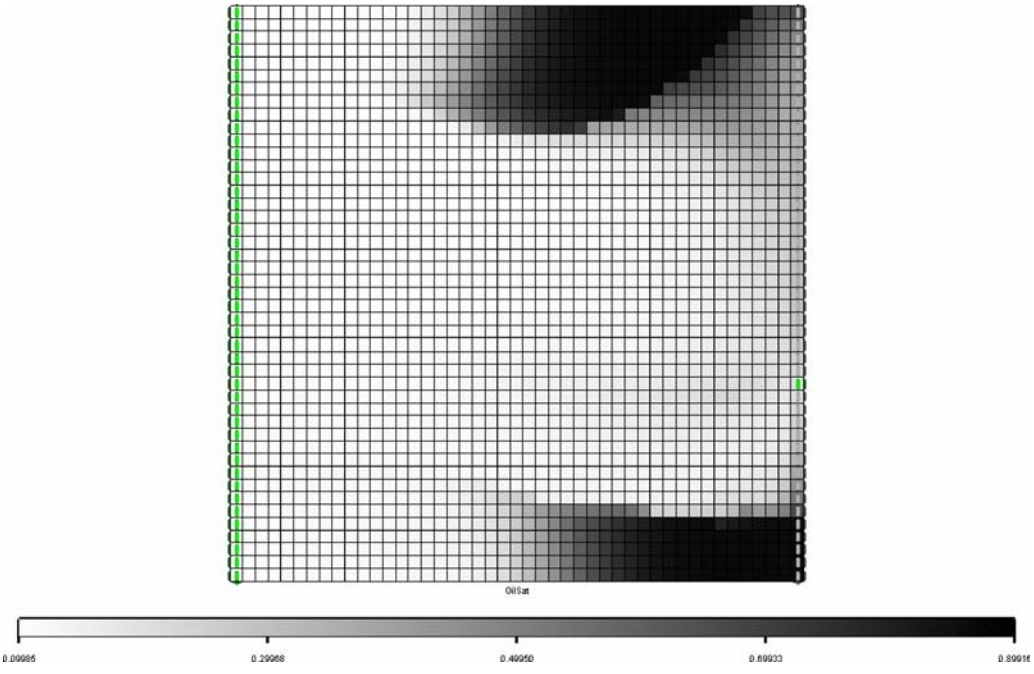

Figure 16. Final oil saturations after one PV injection for optimization with model updating using second approach.

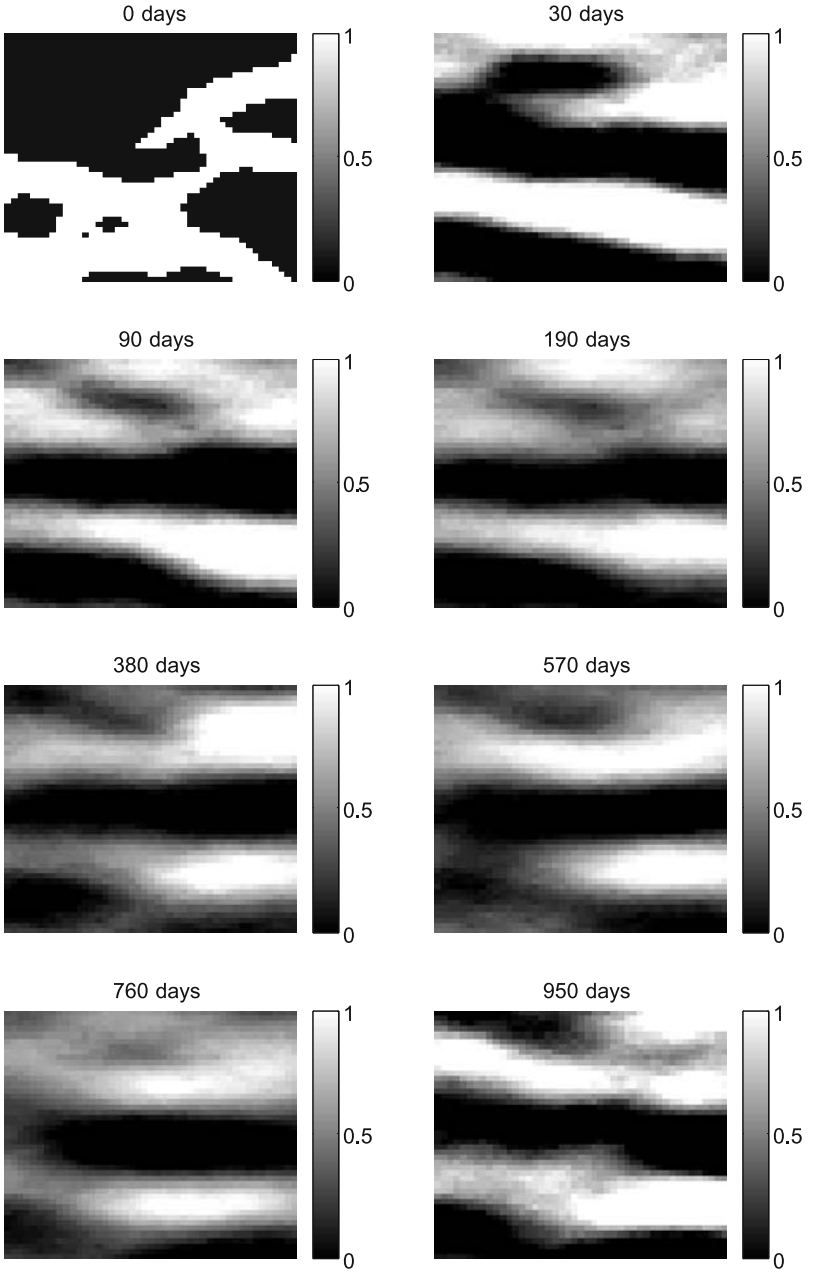

Figure 17. Permeability field updates with model updating performed by assimilating data only over the last control step and with prior term in objective.

clear that the optimal control trajectories obtained are reasonably similar with the open-loop and closed-loop approaches, which is why the sweeps are comparable.

Figure 16 shows the final oil saturations obtained using the second variant of the closed-loop approach. The sweep obtained is even better than the first variant and is very close to that obtained with the open-loop approach. This improvement is due to improved permeability updates. This is evident through comparison of the permeability updates using the second variant (figure 17) with those using the first variant (figure 12). Thus the second approach to model updating is not only more efficient, but seems to provide better model updates by preventing overfitting. The control trajectories (figures 18 and 19) again resemble those using the open-loop approach.

Since the reservoir model and the "true" permeability field are similar to that used by Brouwer et al. [4], a qualitative comparison can be made between the model-updating approach followed here and their use of Kalman filters for the same purpose. Comparing figure 17 with figure 4 of Brouwer et al. [4], it is obvious that the channel structure is much more visible with the present approach. However, this is more likely due to the use of a better prior model (channel training image compared to a Gaussian prior) than to any underlying advantage of the method itself. In any case, given that the objective at hand is to determine the posterior uncertainty of the parameters only, minimization with adjoints seems to be more efficient, as the number of simulations required for convergence is usually around 20–30, whereas with the ensemble Kalman

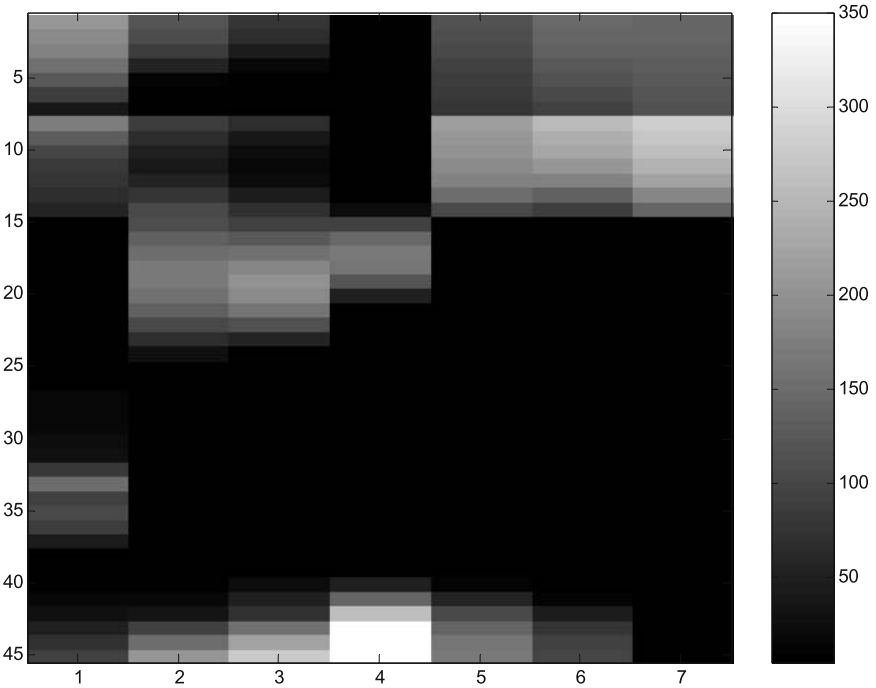

Figure 18. Injection rate variation with time for optimization with model updating using second approach.

filter, about 100–200 forward simulations are required [4, 6]. However, the two methods are not exactly equivalent, as the Kalman filter can also provide the uncertainty in the states.

Figure 20 shows that there is a substantial increase in cumulative oil production with both the open-loop (70%) and closed-loop (60%) approaches, whereas water production is not much affected. This is directly attributable to improved sweep. The increase in NPV is about 100% for the open loop and 85% for the closed loop. The second variant of the closed-loop approach is now applied to another, more geologically complex, example (realization 22, shown in figure 4). Compared to realization 9, this model is more sinuous and the channels are also laterally connected. In this case, the initial model is again taken to be realization 8. The final oil saturations for the uncontrolled case, the open loop, and the closed loop are shown in figures 21, 22 and 23. The evolution of the model is shown in figure 24. Due to the better connectivity of the channels, the final sweep even in the uncontrolled case is considerable. Figure 25 compares the cumulative oil and cumulative water produced. The increase in oil production is around 25% for both the open-loop and closed-loop cases, but there is also an increase in water production by around 30%. The increase in NPV is approximately 25% for both cases.

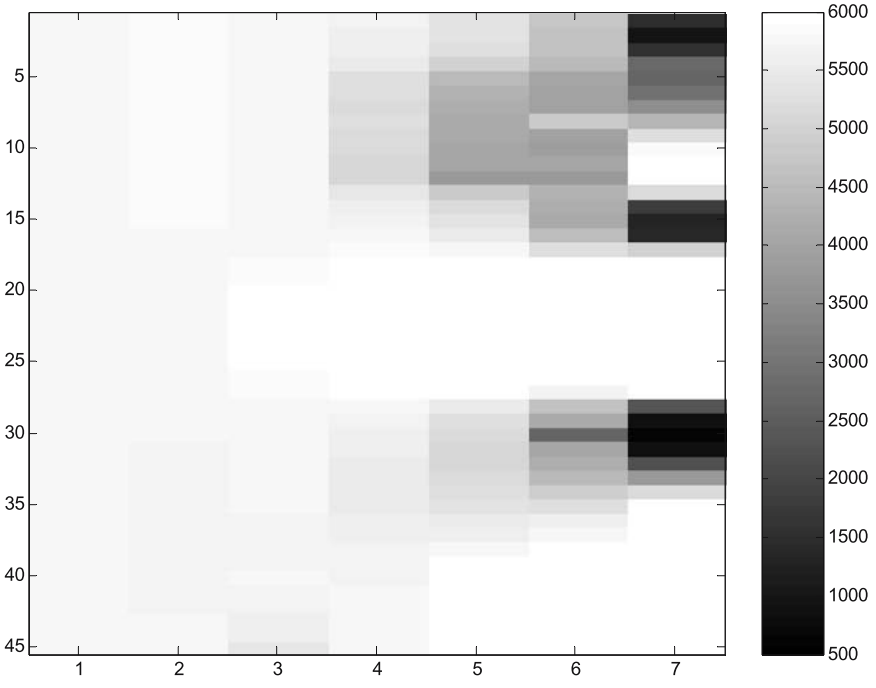

Figure 19. Producer BHP variation with time for optimization with model updating using second approach.

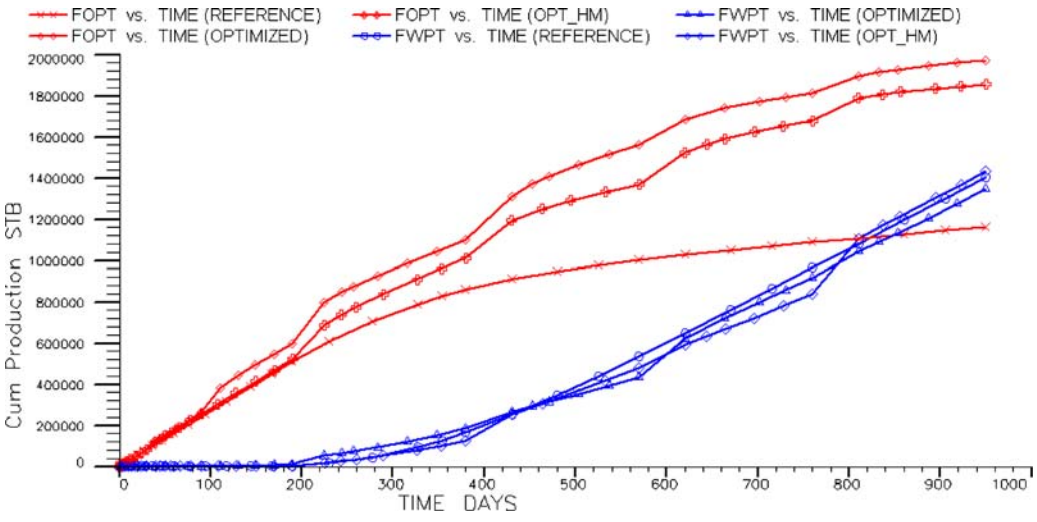

Figure 20. Comparison of cumulative production of oil (FOPT) and water (FWPT) for reference case (REFERENCE), optimized case run with "true" realization (OPTIMIZED), and closed-loop approach (OPT_HM).

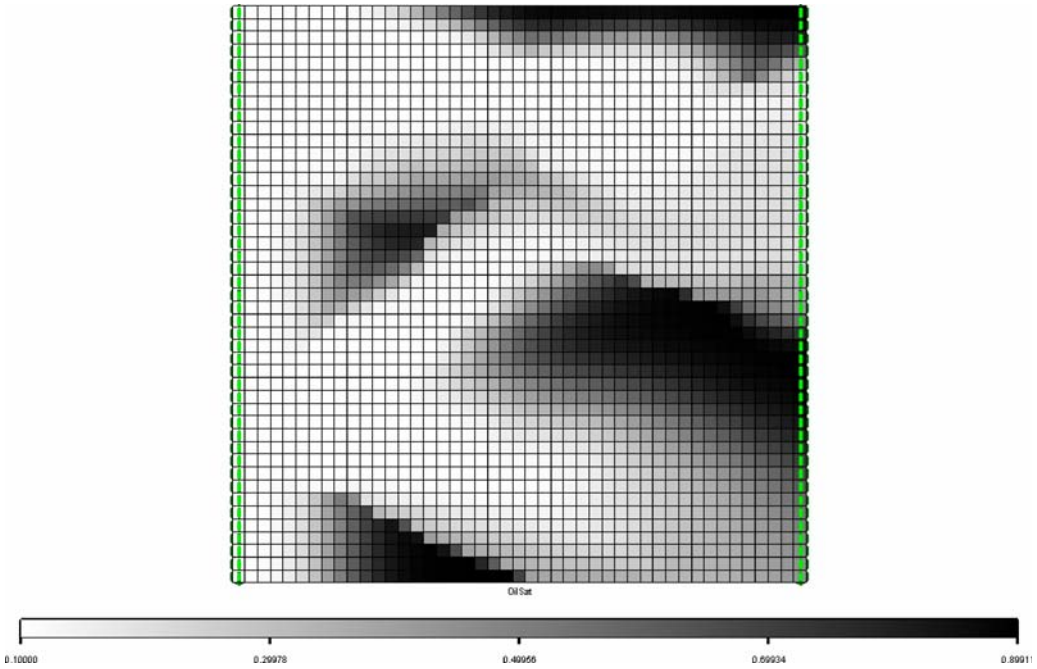

Figure 21. Final oil saturation for uncontrolled reference case (case 2).

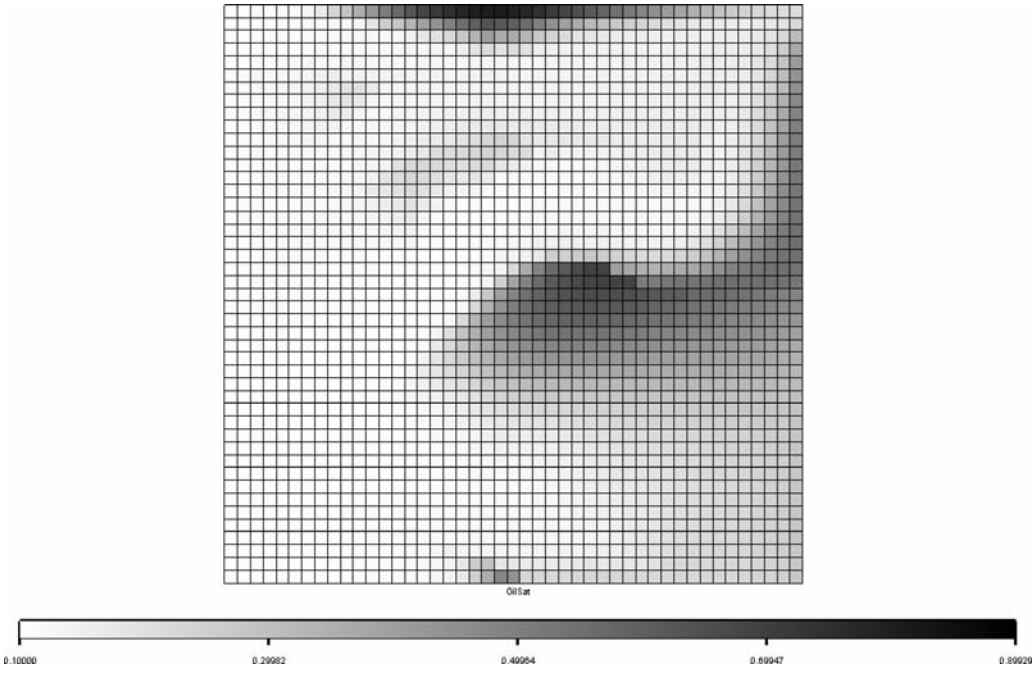

Figure 22. Final oil saturation for optimization on "true" realization (case 2).

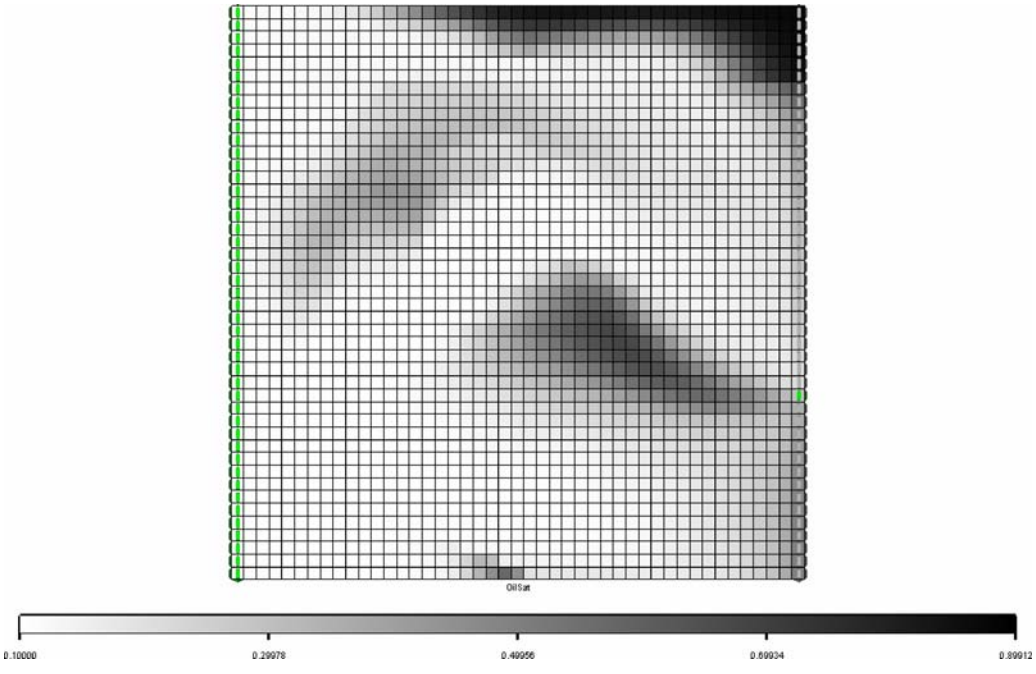

Figure 23. Final oil saturation for optimization with model updating (case 2).

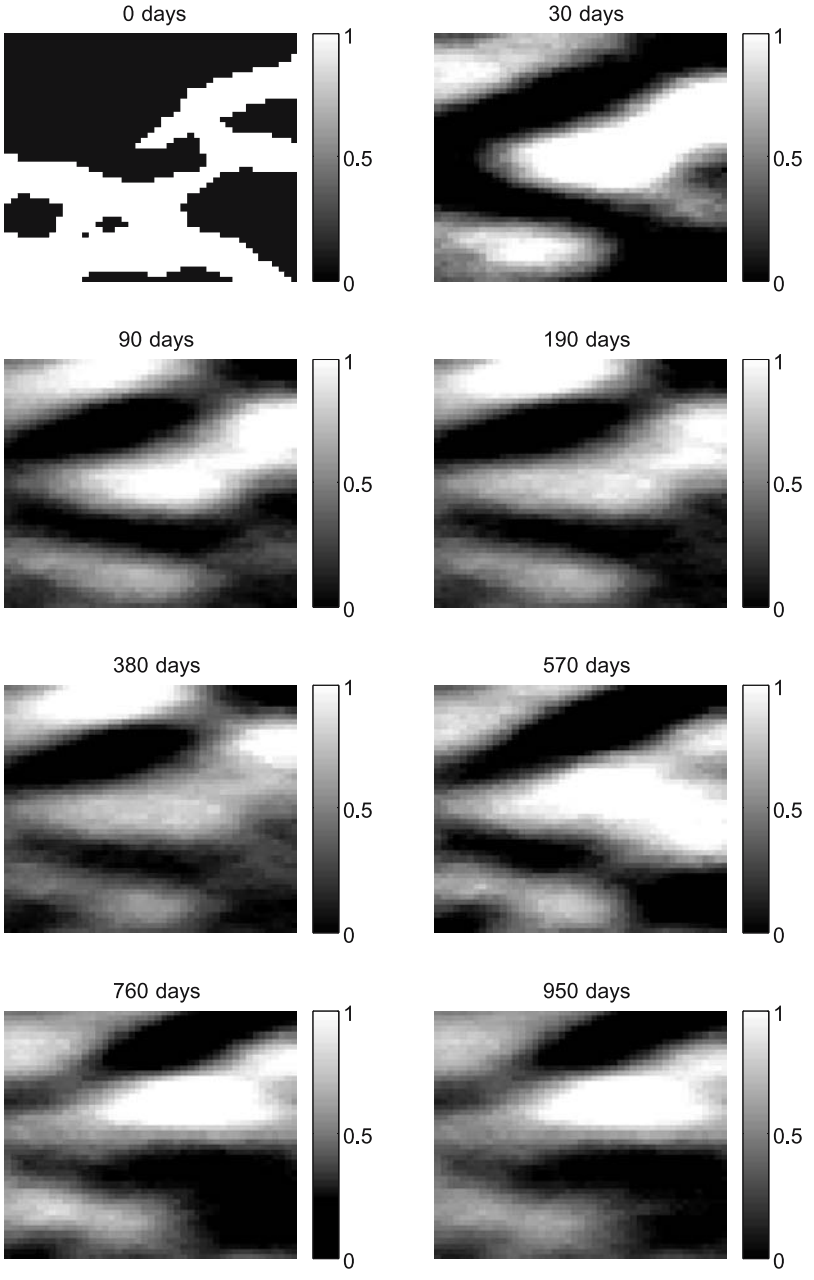

Figure 24. Permeability field updates with model updating performed by assimilating data only over last control step and with prior term in objective (case 2).

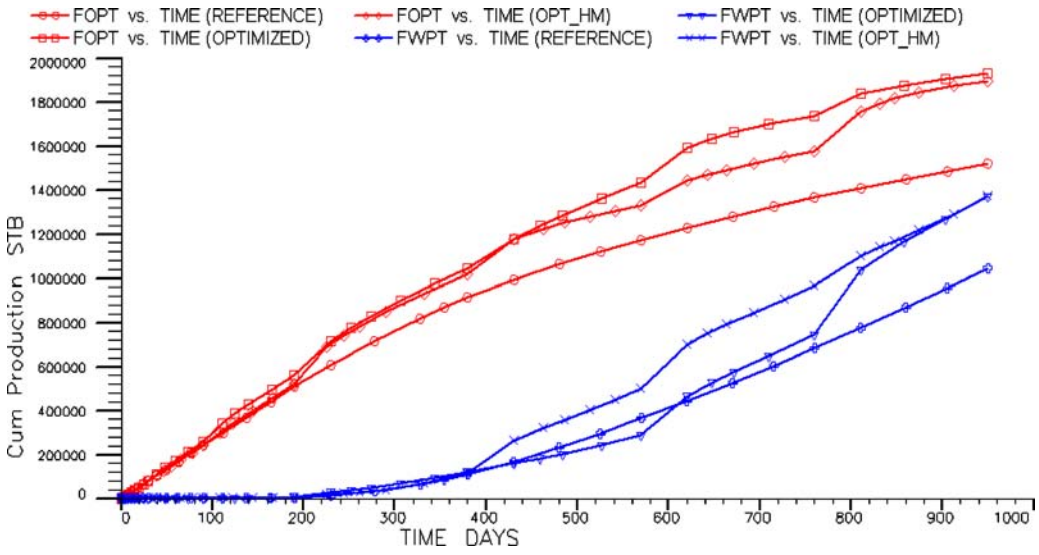

Figure 25. Comparison of cumulative production of oil (FOPT) and water (FWPT) for reference case (REFERENCE), optimized case run with "true" realization (OPTIMIZED), and closed-loop approach (OPT_HM) for case 2.

It is interesting to note that although the model updates, as seen in figure 24, are not as accurate as in the previous case, the closed-loop results are quite close to those obtained via the open-loop approach. This seems to suggest that even very approximate permeability updates may result in nearly correct optimal trajectories, leading to improvements of the objective similar to those obtained using an open loop. The poorer permeability updates can be understood by observing that only very small regions in the training image have similar sinuosity and connectivity as realization 22, implying that realizations similar to realization 22 are relatively rare in the parameter space. This is in contrast to realization 9, which resembles the training image and other realizations more closely, and was as a result better matched during the course of the permeability updates.

8. Conclusions

In this article, the use of adjoint-based models was shown to be very efficient for closed-loop optimal control, and significant improvements in recovery appear to be possible through the application of such techniques. In particular, the following may be concluded:

1. Efficient parameterization of the uncertain reservoir properties in terms of the K–L expansion, combined with Bayesian inversion and adjoint models, provides an efficient algorithm for model updating under geological constraints.

2. The increase in NPV and sweep efficiency by the closed-loop approach is very close to that obtained using an open-loop approach for both of the examples studied. In addition, the results from both examples indicate that approximate parameter fields may be adequate for obtaining near-optimal trajectories of the controls.
3. Assimilating only the new production data at any control step (coupled with the use of the prior term in the history-matching objective function) is much more efficient, and may be as effective as assimilating all existing data.
4. Since adjoint models are used both for optimization and model updating, many components of the code can be reused, resulting in added efficiency.

An important issue that has not been investigated here is the propagation of uncertainty and its effect on the optimal trajectories. Although for the relatively simple cases studied here uncertainty propagation may not be necessary, it can be important for more complex geological scenarios (as demonstrated in [7]). We also need to explore whether preserving two-point statistics is sufficient for the purpose of optimal control under complex geological scenarios. These and related issues will be addressed in future work.

Acknowledgements

We thank the industrial affiliates of the Stanford University Advanced Wells Research Consortium (SUPRI-HW) and Chevron for financial support of this work.

References

[1] M.A. Tatang, *Direct Incorporation of Uncertainty in Chemical and Environmental Engineering Systems*, PhD Thesis, Dept. of Chemical Engineering, Massachusetts Institute of Technology, Cambridge, MA (1995).

[2] P. Sarma, L.J. Durlofsky and K. Aziz, Efficient closed-loop production optimization under uncertainty, in: *SPE Paper 94241 Presented at the SPE Europec/EAGE Annual Conference*, Madrid, Spain (2005).

[3] J.D. Jansen, D.R. Brouwer, G. Naevdal and C.P.J.W. van Kruijsdiik, Closed-loop reservoir management, First Break 23 (2005) 43–48.

[4] D.R. Brouwer, G. Naevdal, J.D. Jansen, E.H. Vefring and C.P.J.W. van Kruijsdiik, Improved reservoir management through optimal control and continuous model updating, in: *SPE Paper 90149 Presented at the SPE Annual Technical Conference and Exhibition*, Houston, TX (2004).

[5] G. Naevdal, L.M. Johnsen, S.I. Aanonsen and E.H. Vefring, Reservoir monitoring and continuous model updating using ensemble Kalman filter, in: *SPE Paper 84372 Presented at the SPE Annual Technical Conference and Exhibition*, Denver, CO (2003).

[6] X.H. Wen and W.H. Chen, Real time reservoir model updating using ensemble Kalman filter, in: *SPE Paper 92991 Presented at the SPE Reservoir Simulation Symposium*, Houston, TX (2005).

[7] I. Aitokhuehi and L.J. Durlofsky, Optimizing the performance of smart wells in complex reservoirs using continuously updated geological models, J. Pet. Sci. Eng. 48 (2005) 254–264.

[8] J. Caers, The probability perturbation method: an alternative to traditional Bayesian approaches for solving inverse problems, presented at *9th European Conference on the Mathematics of Oil Recovery*, Cannes, France (2004).

[9] P.E. Gill, W. Murray and M. Wright, *Practical Optimization* (Academic Press, New York, 1982).

[10] Z. Faithi and W.F. Ramirez, Optimization of an enhanced oil recovery process with boundary controls – a large scale nonlinear maximization, Presented at the *4th IFAC Symposium on Control of Distributed Parameter Systems*, Los Angeles, CA (1985).

[11] G. Mehos and W.F. Ramirez, Use of optimal control theory to optimize carbon dioxide miscible flooding enhanced oil recovery, J. Pet. Sci. Eng. (1989) 247–260.

[12] W. Liu and W.F. Ramirez, Optimal control of three-dimensional steam flooding process, J. Pet. Sci. Eng. (1994) 137–154.

[13] I.S. Zakirov, S.I. Aanonsen, E.S. Zakirov and B.M. Palatnik, Optimization of reservoir performance by automatic allocation of well rates, Presented at the *5th European Conference on the Mathematics of Oil Recovery*, Leoben, Austria (1996).

[14] H. Asheim, Maximization of water sweep efficiency by controlling production and injection rates, in: *SPE Paper 18365 Presented at the SPE European Petroleum Conference*, London, UK (1988).

[15] G.A. Vironovsky, Waterflooding strategy design using optimal control theory, Presented at the *6th European IOR Symposium*, Stavanger, Norway (1991).

[16] B. Sudaryanto and Y.C. Yortsos, Optimization of displacements in porous media using rate control, in: *SPE Paper 71509 Presented at the SPE Annual Technical Conference and Exhibition*, New Orleans, LA (2001).

[17] D.R. Brouwer and J.D. Jansen, Dynamic optimization of water flooding with smart wells using optimal control theory, SPEJ. (Dec 2004) 391–402.

[18] W.H. Chen, G.R. Gavalas, J.H. Seinfeld and M.L. Wasserman, A new algorithm for automatic history matching, SPEJ. 14 (1974) 593–608.

[19] G.M. Chavent, M. Dupuy and P. Lemonnier, History matching by use of optimal control theory, SPEJ. 15 (1975) 74–86.

[20] M.L. Wasserman, A.S. Emanuel and J.H. Seinfeld, Practical applications of optimal control theory to history-matching multiphase simulator models, in: *SPE Paper 5020 Presented at the SPE–AIME Annual Fall Meeting*, Houston, TX (1974).

[21] A.T. Watson, J.H. Seinfeld, G.R. Gavalas and P.T. Woo, History matching in two-phase petroleum reservoirs, in: *SPE Paper 8250 Presented at the SPE–AIME Annual Fall Technical Conference and Exhibition*, Las Vegas, NV (1979).

[22] Z. Wu, A.C. Reynolds and D.S. Oliver, Conditioning geostatistical models to two-phase production data, SPEJ. 4 (1999) 142–155.

[23] R. Li, A.C. Reynolds and D.S. Oliver, History matching of three-phase flow production data, in: *SPE Paper 66351 Presented at the SPE Reservoir Simulation Symposium*, Houston, TX (2001).

[24] Z. Wu and A. Datta-Gupta, Rapid history matching using a generalized travel time inversion method, in: *SPE Paper 66352 Presented at the SPE Reservoir Simulation Symposium*, Houston, TX (2001).

[25] F. Zhang, J.A. Skjervheim, A.C. Reynolds and D.S. Oliver, Automatic history matching in a Bayesian framework, example applications, in: *SPE Paper 84461 Presented at the SPE Annual Technical Conference and Exhibition*, Denver, CO (2003).

[26] G.R. Gavalas, P.C. Shah and J.H. Seinfeld, Reservoir history matching by Bayesian estimation, SPEJ. 16 (1976) 337–350.

[27] D.S. Oliver, Multiple realizations of the permeability field from well test data, SPEJ. 1 (June 1996) 145–154.

[28] A.C. Reynolds, N. He, L. Chu and D.S. Oliver, Reparameterization techniques for generating reservoir descriptions conditioned to variograms and well-test pressure data, SPEJ. 1 (Dec 1996) 413–426.

[29] P. Sarma, K. Aziz and L.J. Durlofsky, Implementation of adjoint solution for optimal control of smart wells, in: *SPE Paper 92864 Presented at the SPE Reservoir Simulation Symposium*, Houston, TX (2005).

[30] R.F. Stengel, *Optimal Control and Estimation* (Dover Publications, New York, 1985).

[31] A. Tarantola, *Inverse Problem Theory* (Soc. Ind. Appl. Math., Philadelphia, 2005).

[32] S.P. Huang, S.T. Quek and K.K. Phoon, Convergence study of the truncated Karhunen–Loeve expansion for simulation of stochastic processes, Int. J. Numer. Methods Eng. 52 (2001) 1029–1043.

[33] M. Loeve, *Probability Theory I and II*, 4th Edition (Springer-Verlag, New York, 1977).

[34] J.K. Cullum, *Lanczos Algorithms for Large Symmetric Eigenvalue Computations* (Birkhauser, Boston, 1985).

[35] S. Strebelle, Conditional simulation of complex geological structures using multiple-point statistics, Math. Geol. 34 (2002) 1–22.